Renewable Energy 222 (2024) 119973

Contents lists available at ScienceDirect

Renewable Energy

journal homepage: www.elsevier.com/locate/renene

A novel python-based floating offshore wind turbine simulation framework

Javier López-Queija [a,b,*], Eneko Sotomayor [c], Josu Jugo [c], Ander Aristondo [a], Eider Robles [a,d]

[a] TECNALIA, Basque Research and Technology Alliance (BRTA), Parque Tecnológico de Bizkaia, Astondo Bidea, Edificio 700, E-48160, Derio, Bizkaia, Spain
[b] Mechanical Engineering Department, University of the Basque Country UPV/EHU, Bilbao, 48013, Spain
[c] Electricity and Electronics Department, University of the Basque Country UPV/EHU, Leioa, 48940, Spain
[d] Automatics and System Engineering Department, University of the Basque Country UPV/EHU, Bilbao, 48013, Spain

ARTICLE INFO

Keywords:
Floating offshore wind turbines
Wind turbine modelling
Offshore dynamics
Aerodynamics
Hydrodynamics
Structural dynamics
Mooring dynamics
Wind turbine control
Wind energy

ABSTRACT

The expansion of floating offshore wind brings the industry closer to achieving commercial viability. However, the challenging environment characterised by strong winds, waves, and currents, along with the growing size of wind turbines and the dynamic behaviour of floaters, introduces concerns about power production efficiency and system durability due to increased fatigue loads, which subsequently impacts overall costs. In an attempt to mitigate the financial implications coming from alterations made to control strategies and structural elements during the initial design phase, this paper propounds an all-encompassing simulation framework for offshore wind turbines. The current study thoroughly explores the various capabilities of the tool, with a focus on its simulation models. Importantly, the paper highlights the complex interactions between tool models and different controllers. Carefully designed, this tool offers users a variety of functions to enhance system design, fine-tune control strategies, and thoroughly assess performance metrics. The paper elaborates on these aspects, providing an explanation of the tool's capabilities and enhancing the dynamic comparison between the models.

1. Introduction

In recent years, there has been a significant increase in investment and research efforts dedicated to floating offshore wind turbine (FOWT) technology. This growing interest has been observed across academia and the industry alike. The potential benefits and advantages of FOWTs, such as their ability to harness wind energy in deeper waters and access more favourable wind resources [1], have attracted substantial attention and resources. As a result, there has been a surge in research, development, and innovation in the field, with the aim of advancing FOWT technology and unlocking its full potential in the renewable energy sector [2]. However, the Levelized Cost of Energy (LCOE) is still high [3].

Traditionally, the design process for the actual FOWTs has followed a sequential approach, where the controller design and optimization are typically carried out towards the later stages of the overall design process. Neglecting the inherent coupling between system dynamics and controller behaviour by treating the controller design as an independent component can result in suboptimal solutions [4]. To address this limitation, a more integrated approach is needed where the controller design is considered concurrently with the overall system design. This approach, commonly known as control co-design (CCD), recognises the coupling between the system and control dynamics, allowing for the optimization of both aspects in a synergistic manner [5]. In Ref. [6], a comprehensive review of the latest frameworks for the optimization procedure is presented, providing insights into their features, functionalities, and classification.

An example of such a tool is the Wind Energy with Integrated Servo-control (WEIS [7]) developed at the National Renewable Energy Laboratory (NREL). WEIS facilitates multi-fidelity CCD of wind turbines based on various NREL tools for assembly assessment [8,9] and simulation [10,11]. Nevertheless, it is important to note that the available controllers during the optimization procedure are currently limited to proportional-integral (PI) controllers. Some researchers developed tools for quick optimization procedures. For instance, in Ref. [12] where a linear parameter varying model is used to perform the FOWT system optimization with an open-loop control approach. On the other hand, in Ref. [13] a linear reduced order frequency domain model is used during the optimization process. Although, none of them includes more complex models for optimum design validation.

In this work, a new and versatile floating wind turbine design tool framework is proposed. The proposed design framework is built upon the combination of a reduced order time domain dynamic model and a

* Corresponding author. TECNALIA, Basque Research and Technology Alliance (BRTA), Parque Tecnológico de Bizkaia, Astondo Bidea, Edificio 700, E-48160, Derio, Bizkaia, Spain.

E-mail address: javier.lopez@tecnalia.com (J. López-Queija).

https://doi.org/10.1016/j.renene.2024.119973
Received 21 August 2023; Received in revised form 2 January 2024; Accepted 8 January 2024
Available online 9 January 2024

Nomenclature

BEM	Blade element momentum
CB	Buoyancy centre
DLC	Design load case
DLL	Dynamic link library
DOF	Degree of freedom
FOWT	Floating offshore wind turbine
LCOE	Levelized cost of energy
MBS	Multibody system
NMPC	Nonlinear model predictive control
OCP	Optimal control problem
PC	Pitch controller
PI	Proportional Integral
PSD	Power spectral density
QTF	Quadratic transfer function
RAO	Response amplitude operator
SQP	Sequential quadratic programming
TC	Torque controller
VSVP	Variable speed variable pitch

more complex nonlinear wind turbine simulation model, providing a seamless transition between the modelling approaches. Additionally, within the proposed design structure different controllers are available including state-of-art and model based advanced controllers. The framework is proposed to serve as an early-stage design decision-making tool where the simplified model serves as system candidate evaluation model while the more complex model is used for the validation. The modular implementation of the proposed decision-making tool allows for different applications: control strategy design, evaluation, and comparison; floating wind turbine system development, evaluation, and validation through different complexity models; optimization of the controller, the system or both simultaneously. The flexibility of the tool offers the user different options that will be covered in different publications. In this study, the focus is on presenting the tool's structure, the available models, and the control options. This is executed by assessing the response of an assumed optimum floating wind turbine system design under various simulation conditions employing the diverse models and controllers available in the tool.

The structure of the publication is as follows: In Section 2, the proposed structure and workflow of the tool is discussed, providing insights into its architecture and how it operates. Section 3 provides a brief overview of the various controllers available within the tool, highlighting their functionalities and capabilities. In Section 4, a comprehensive discussion on the different complexity level models implemented in the tool is derived. Section 5 focuses on the validation of the tool's dynamic performance for the optimization procedure, showcasing its effectiveness and robustness based on the evaluation of the dynamic response of the models. Finally, Section 6 summarises the main contributions of the study and discusses the new features that need to be developed in order to further enhance the tool's capabilities and applicability.

2. Tool workflow and structure

This section outlines the workflow implemented within the tool's structure, providing a detailed description of each step and its corresponding role in the overall process. Fig. 1 illustrates the schematic representation of the proposed structure for the optimization tool. It visually demonstrates the key components and their interconnections within the tool's framework.

The framework code is designed as a modular tool, enabling the inclusion or creation of new control strategies simply by adding a new module. Similarly, users have the flexibility to choose from existing models of varying complexity or develop their own models as needed.

The tool offers two primary control strategies: feedback control and optimal control. Users can choose between various types of controllers, including traditional PI controllers and model-based controllers, or to implement their desired control strategy. The modular nature of the tool allows for seamless integration of different controllers, enabling users to incorporate a wide range of control algorithms and experiment with

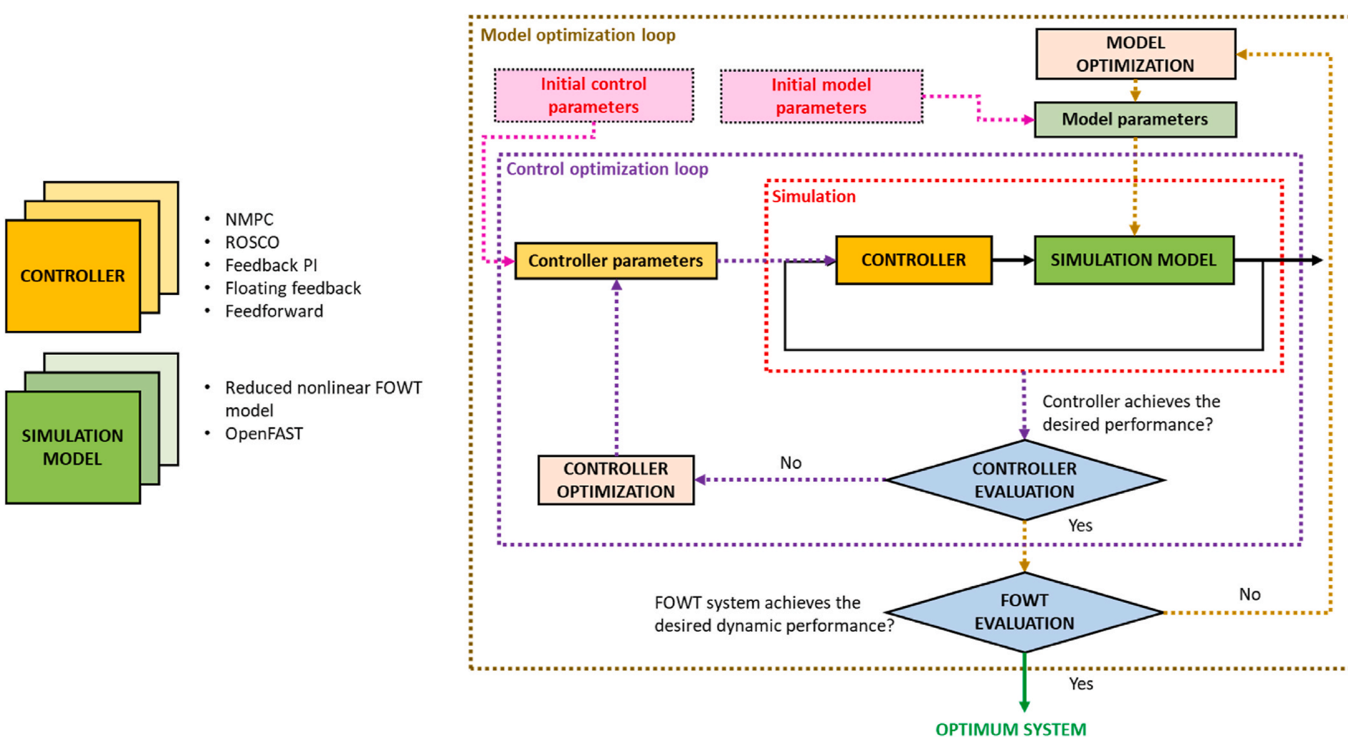

Fig. 1. Tool proposed structure and workflow.

different control techniques based on their specific needs and preferences.

The tool is also designed to accommodate simulation models of varying complexity levels. Currently, it offers two models: a reduced-order time domain nonlinear dynamic FOWT model and OpenFAST [11]. Moreover, the tool provides the flexibility for users to implement their own custom models. This diverse selection of models enables users to perform optimization and evaluation procedures. The simpler model is intended for use in the optimization and control design process, providing efficient computations. On the other hand, the more complex OpenFAST model is utilised for comprehensive evaluation and analysis, capturing a higher level of detail and accuracy after reaching an optimum design.

Both models share a common dataset, enabling seamless and straightforward conversion between them. This means that users can easily switch between the reduced-order time domain nonlinear dynamic FOWT model and OpenFAST without any data compatibility issues, see Fig. 2. The shared data includes important parameters such as environmental conditions and controller settings, ensuring consistency and allowing for efficient evaluation of FOWT models or controllers. The models and controllers are briefly discussed in the respective sections of the publication.

The tool's flexibility and workflow empower users to adapt to specific requirements and objectives during the initial design stages, enabling them to make informed decisions and evolve the concept of the FOWT system. Modifications to the system's characteristics necessitate merely the adjustment of inputs furnished to the designated model. For instance, altering the dimensions of the floater would prompt adjustments in the inputs for the hydrodynamic model, while modifications to mooring lines would warrant changes in the input parameters for the mooring system model.

Whether it's optimizing the controller, refining the system design, or both simultaneously, users have the freedom to explore different options and iterate on their designs. This iterative process facilitates the refinement and improvement of the FOWT system, ensuring that it aligns with the desired performance goals and operational parameters. By accommodating various design considerations and allowing for concurrent exploration of multiple design aspects, the tool supports a comprehensive and dynamic approach to FOWT system development.

The modularity of the tool is achieved through its implementation in Python, utilizing object-oriented programming. Each of the proposed modules is designed as its own class, allowing for easy integration and customization within the tool. For example, the simulation model class encapsulates the dynamics of the model obtained from each of its subclasses, including aerodynamics, hydrodynamics, structural dynamics, and moorings. Similarly, the higher complexity level model OpenFAST has been adapted to function in a similar manner in its Matlab-Simulink version. This adaptation involves providing a data array, which includes the controller actions, to its class for simulation purposes.

3. Controllers for floating offshore wind turbines

The tool offers a variety of controllers within different control strategies that can be selected for the dynamic simulation or the optimization process. It provides options for both feedback-based controllers and model-based controllers, including optimal controls. Additionally, the user can implement and test its desired control strategy by including a new controller within the appropriate class and test those controllers using simulation models of varying complexity levels. In this section, a brief description of the two different controller families available within the tool at this development point is presented.

The tool is compatible with the widely used wind turbine controller ROSCO and its dependencies [14,15]. This allows for running the high-fidelity model with ROSCO and serves as a design and validation tool for the controller designed in the proposed framework with the reduced models. Evaluating and refining controllers with reduced dynamic models and comparing their performance against ROSCO tunings for specific wind turbines in a complex simulation environment allows for different FOWT control research pathways.

3.1. Feedback based controllers

The first family of controllers implemented within the tool consists of feedback-based controllers that are widely used by the research community. Accounting for the negative damping phenomena [16,17] is crucial in the design of feedback-based controllers and, consequently, in the dynamic performance of the system for optimization process. The presence of negative damping necessitates careful consideration to ensure stable and robust control performance. The work conducted in Ref. [18] focuses on identifying and characterizing various

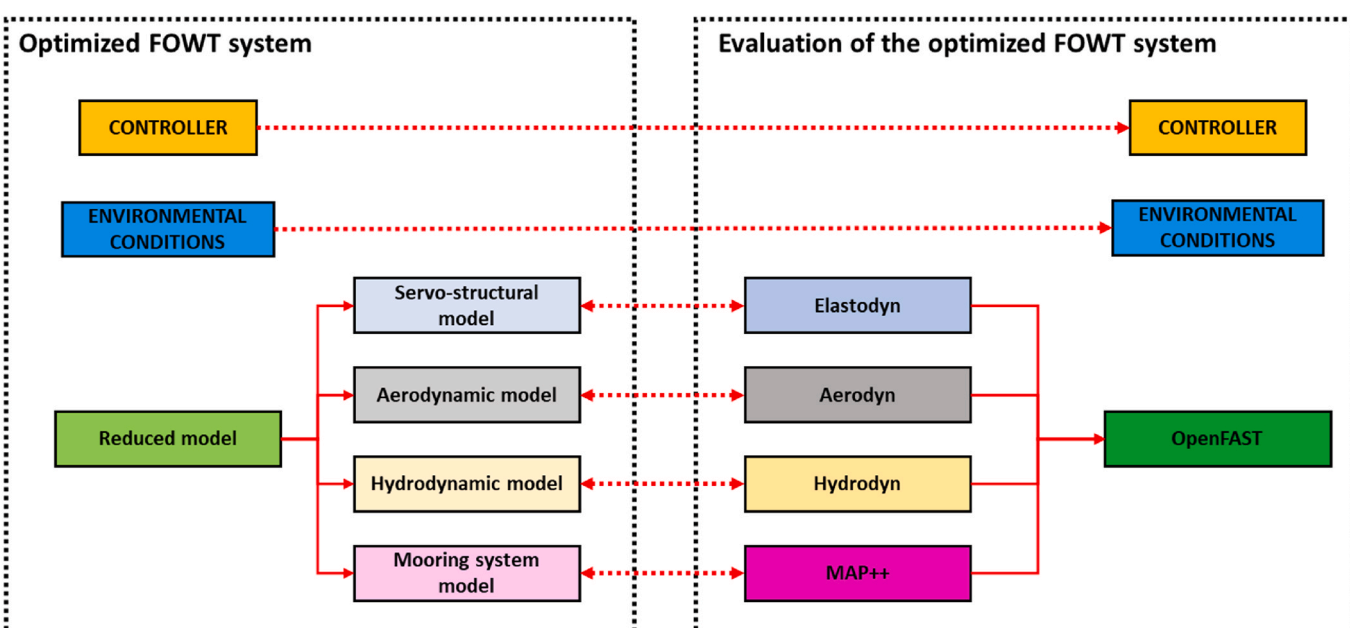

Fig. 2. Common module structure for data sharing between different complexity level models.

feedback-based controllers for FOWTs that are integrated into the proposed framework as conventional controllers. The proposed framework includes many of these controllers, allowing for their integration and utilization within the tool. Furthermore, the Python-based implementation facilitates the effortless inclusion of any controller being developed by the user.

Modern wind turbines operate with variable speed and variable pitch operation modes, enabling control over both the generator torque and the blade pitch angle controllers [19]. The selection of the active controller during operation is based on the wind speed falling within a predefined range, ensuring that a specific objective is met. Below the rated wind speed, the torque controller is responsible for maximizing power extraction from the wind. However, above the rated wind speed, the blade pitch angle controller faces the challenge of balancing two competing objectives. On one hand, it needs to regulate the rotor speed to its rated value, while on the other hand, it must stabilise the platform to ensure safe and efficient operation [20,21].

The proposed feedback-based FOWT controllers adopts these very same features, aligning with industry standards and criteria. It incorporates various proportional-integral (PI) regulators, as depicted in equation (1), to optimise the performance of the overall FOWT system.

$$T^{c}_{gen} = K^{TC}_{p} \cdot \left(\Delta\Omega + \frac{1}{T^{TC}_{i}}\Delta\Omega\right) \qquad [1]$$

$$\theta^{c}_{col} = K^{PC}_{p} \cdot \left(\Delta\Omega + \frac{1}{T^{PC}_{i}}\Delta\Omega\right) \cdot GS(v_0)$$

Where the K_p and T_i are the proportional gain and the integral time for the torque controller (TC) and the collective blade pitch controller (PC) respectively. Wind turbine systems exhibit nonlinearity in variable pitch operations beyond rated winds. To address this, a gain scheduled strategy is incorporated through the term $GS(v_0)$ utilizing an interpolation of precalculated gains. The role of the regulator is to minimise the rotor speed error ($\Delta\Omega$) by adjusting the system to the reference rotor speed. T^{c}_{gen} and θ^{c}_{col} are the commanded torque and pitch control actions calculated by the regulator.

The first implementation is a simple feedback PI controller which above rated windspeed, incorporates a detuning procedure to reduce the controller bandwidth below the natural frequency of the pitch rigid solid motion of the FOWT [16,22]. By reducing the gains of the controller, the response to the rigid pitch motion of the system is dampened, resulting in improved stability during operation above the rated wind conditions [20].

A second feedback loop can be integrated into the FOWT system control tool. This controller builds upon the previous one, but with the addition of the tower top velocity signal ($\dot{x}_T$) or the rigid solid FOWT pitch motion ($\dot{\varphi}$) to modify the blade pitch control action ($-K_d \cdot \dot{x}_T$ or $-K_d \cdot \dot{\varphi}$), as proposed in Ref. [14] or [17]. By incorporating the tower top velocity or the FOWT pitch motion signal into the control algorithm, the pitch control action can be adjusted in real-time based on the current measured signal, see equation (2).

$$\theta^{c}_{col} = K^{PC}_{p} \cdot \left(\Delta\Omega + \frac{1}{T^{PC}_{i}}\Delta\Omega\right) \cdot GS(v_0) - K_d \cdot \dot{x}_T \qquad [2]$$

The last control loop that can be included is a feedforward control loop. The fundamental concept of feedforward control, as proposed in Ref. [23], is incorporated as control option into the proposed tool framework. This concept involves anticipating the effects of external disturbances, wind and waves in the case of FOWT, or changes in the system and applying appropriate control actions $\theta_{FF}(v_0)$. in advance to mitigate their impact.

$$\theta^{c}_{col} = K^{PC}_{p} \cdot \left(\Delta\Omega + \frac{1}{T^{PC}_{i}}\Delta\Omega\right) \cdot GS(v_0) - K_d \cdot \dot{x}_T + \theta_{FF}(v_0) \qquad [3]$$

3.2. Optimal controllers

The tool also includes a second family of controllers based on optimal control theory. Among the implemented controllers, various complexity level nonlinear model predictive controllers (NMPC) can be chosen. These controllers utilise the reduced order dynamic model integrated within the tool as internal model to calculate the optimal control actions by solving an optimal control problem (OCP) over a predefined time horizon. The objective of the optimal control problem for a FOWT system is to determine the optimal control trajectory $u(\cdot)$ that minimises a cost function J_{OCP}. The optimization problem is defined by J_{OCP} as the integral of an objective function (F) over the predicted time horizon (T_f) evaluated from current time (t_0) to the final time. The reduced nonlinear time domain FOWT model is used along with a set of constrains ($t_0 + T_f$) to formulate the problem as presented in equation (4).

$$\min_{u(\cdot)} J_{OCP}$$

$$\text{with} : J_{OCP} = \sum\nolimits_{t_0}^{t_0+T_f} F(x(\tau), u(\tau), d(\tau))\, d\tau$$

$$\text{subjected to} \quad \begin{array}{c} \dot{x} = f(x, u, d) \\ x(t_0) = x_0 \\ H(x(\tau), u(\tau), d(\tau)) \geq 0 \; \forall \tau \in [t_0, t_0 + T_f] \end{array} \qquad [4]$$

The cost function for the NMPC is formulated as a quadratic function by the user. So, different cost functions can be easily implemented to compare their performance. The objective function's weights are assumed to be independent of the system states (x) and inputs (u), while they may depend on external disturbances (d). The OCP is solved using sequential quadratic programming (SQP) by iteratively transforming it into a nonlinear program [24,25]. In the current implementation the tool employs ACADOS [26,27] as the SQP solver to obtain solutions for the OCP.

4. Dynamic floating offshore wind turbine models

In the proposed optimization framework, a range of complexity level models can be employed. For the optimised system validation a complex dynamic model, OpenFAST [11], supported by NREL, is used. While the system dimensions and controllers optimization process utilises a low complexity dynamic model based on the work in Ref. [28]. Additionally, the tool's modular framework enables users to easily incorporate any other FOWT model of their choice. In this study, the dynamic performance of the low complexity model is compared with the more complex OpenFAST model to validate the suitability of the low complexity model for optimization processes.

4.1. OpenFAST dynamic model

As discussed in Section 2, a more comprehensive dynamic time domain model is required to validate the optimised designs obtained. In this initial version of the tool, OpenFAST [11], supported by NREL, is utilised for this purpose. OpenFAST is a multi-physics, multi-fidelity tool for simulating the coupled dynamic response of wind turbines, both onshore and floating. The code is integrated with modules that encompass aerodynamics, hydrodynamics for offshore foundations, control, and electrical system dynamics, as well as structural dynamics, enabling nonlinear time domain simulations.

The Aerodyn module [10], integrated within OpenFAST, accurately calculates aerodynamic loads using actuator line principles. It approximates 3D flow around turbine components by considering local 2D flow at cross sections. The module incorporates lift and drag forces, pitching moments, and various options for rotor wake, airfoil aerodynamics, tower influence, tower drag, and aeroacoustics. It is based on the Blade Element Momentum (BEM) theory [29].

The Inflowind module [10], integrated into the OpenFAST model, plays a vital role in processing the wind inflow. It provides the necessary functionality to simulate a wide range of wind conditions, such as steady winds, constant winds, and turbulent winds. The module accurately calculates the wind speeds, which are then used as inputs in the aerodynamic module to compute the loads on the wind turbine.

Elastodyn is the structural dynamics module in OpenFAST, simulating the dynamic behaviour of components like blades, drivetrain, nacelle, and tower. It uses multibody theory (MBS) and modal approximation techniques [30] to model flexible subcomponents, ensuring accurate representation of dynamic response and deformations. The model incorporates multiple degrees of freedom to capture the system's behaviour, including blade modes, drivetrain flexibility, generator speed, wind turbine system yaw motion, tower modes, and foundation modes.

The Hydrodyn module [10] in OpenFAST handles the dynamics of offshore foundations, considering hydrodynamic forces and interactions with water. It utilises various methods to calculate hydrodynamic loads, including potential-flow theory, strip-theory, and a hybrid approach combining both. HydroDyn is capable of generating different types of waves, such as regular or irregular waves, and long-crested or short-crested waves, representing wave energy in different directions. It internally generates waves using analytical methods for finite depth, incorporating first-order or first plus second-order wave theory [31,32].

OpenFAST provides various modules for mooring analysis [10]. In the proposed tool, the OpenFAST model utilises a steady-state approximation to estimate the forces in the multi-segmented mooring lines [33]. The mooring model employed in OpenFAST is based on conventional single-line static solutions. It solves the algebraic equation for all mooring line elements simultaneously, ensuring that the total force at the connection points balances to zero. The module also allows for modelling seabed contact, seabed friction, and external forces.

The control module in OpenFAST, known as Servodyn, provides the functionality to define and implement controllers within the simulation. The module interacts with a dynamic link library (DLL) where the controller logic is programmed or interfaces with Matlab-Simulink. In the proposed tool, similar capabilities for Matlab-Simulink integration have been developed using the suite of Python tools to work with OpenFAST, enabling the use of advanced control strategies and algorithms within the simulation framework.

4.2. Reduced time domain dynamic model

In this subsection, a comprehensive description is provided for the nonlinear time domain dynamic model that has been developed and employed within the proposed tool framework as low complexity model. In the same way, different models with more or less DOFs can be used during simulation or the optimization process as well as for the internal model of the model-based controllers. The presented model for this publication is the most complicated low complexity level available model within the tool including all the floating DOFs interacting with the controller so it can serve as a fundamental component for accurate simulation and analysis of the FOWT system.

4.2.1. Servo – structural model

The model developed in Ref. [28] follows a control-oriented wind turbine model using the MBS approach, as explained in Ref. [19]. This approach allows for low-order modelling by considering only the DOFs directly coupled with the controller design. During variable-speed variable-pitch (VSVP) operation of a wind turbine, the speed control mechanism interacts with modes in the rotation frame. These modes include the drivetrain torsion mode and blade edgewise bending modes. However, it is important to note that the natural frequencies of these modes are typically beyond the bandwidth frequency of the controller [19]. This characteristic allows for simplification in the FOWT model, Fig. 3.

The FOWT system is modelled as a two-lumped mass system, where the masses represent the foundations and the rotor nacelle assembly. These two masses are connected by a flexible beam representing the tower. The dynamics of the FOWT system are characterised by considering the interaction between rotor and along-wind FOWT system modes. In floating wind operation, the surge (u) and pitch (φ) modes have been identified in Ref. [34] as the most critical modes for FOWT controllers. These modes are particularly important due to the occurrence of negative damping phenomena, which can significantly impact the stability and performance of the system [16,22]. The model also accounts for the first fore – aft tower mode (x_T) due to its low natural frequency significantly excited by aerodynamic thrust force.

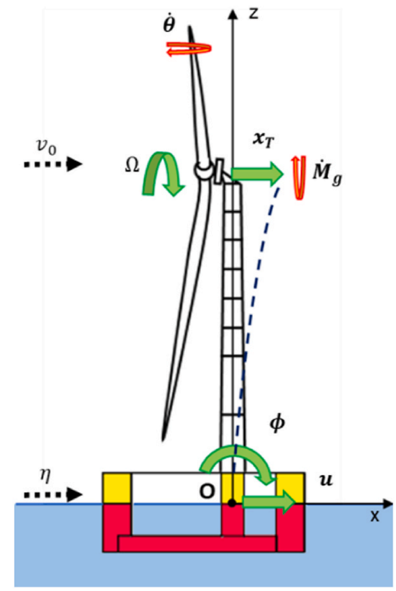

Fig. 3. DOFs utilised within the reduced nonlinear dynamic model.

$$\boldsymbol{q} = \begin{bmatrix} u \\ \varphi \\ x_T \\ \Omega \end{bmatrix} \qquad [5]$$

Applying Newton's second law the equation of motion of the FOWT system can obtained:

$$[\boldsymbol{M}] \cdot \ddot{\boldsymbol{q}} + [\boldsymbol{C}] \cdot \dot{\boldsymbol{q}} + [\boldsymbol{K}] \cdot \boldsymbol{q} = \boldsymbol{F}_{ext} \qquad [6]$$

Unlike most existing models, the proposed model takes into account the dynamics of the actuators for the generator torque ($\dot{T}_g$) and blade pitch angle ($\dot{\theta}$) operational control, in a simplified way. The coupled system can be written in state-space formulation as follows:

$$\begin{bmatrix} \dot{\boldsymbol{q}} \\ \ddot{\boldsymbol{q}} \\ \dot{T}_g \\ \dot{\theta} \end{bmatrix} = \begin{bmatrix} \dot{\boldsymbol{q}} \\ [\boldsymbol{M}]^{-1}[-[\boldsymbol{C}]\cdot\boldsymbol{q} - [\boldsymbol{K}]\cdot\boldsymbol{q} - \boldsymbol{F}_{ext}] \\ \frac{1}{\tau_{T_g}}\cdot\left(T_g^c - T_g\right) \\ \frac{1}{\tau_\theta}\cdot(\theta^c - \theta) \end{bmatrix} \qquad [7]$$

Where $[\boldsymbol{M}]$, $[\boldsymbol{C}]$ and $[\boldsymbol{K}]$ are the system mass, damping and stiffness matrixes, details about those matrices can be found in Ref. [28]. The external forces, labelled as $\boldsymbol{F}_{ext}$, encompass environmental conditions through aerodynamic and hydrodynamic models, as well as mooring forces. These loads are computed using distinct models described in the subsequent subsections.

4.2.2. Aerodynamic model

The integrated aerodynamic model within the reduced FOWT model for wind – turbine interaction representation is based in the BEM theory [29]. To alleviate the computational burden associated with the iterative calculation of lift and drag forces, a simplified aerodynamic model is developed. This aerodynamic model is based on the power and thrust coefficient surfaces, as shown in Fig. 4, which define the aerodynamic properties of the wind turbine. By using this simplified approach, the computational requirements are reduced while still capturing the essential aerodynamic characteristics of the system.

The surfaces are pre-processed using the same aerodynamic module from OpenFAST for different tip-speed-ratios (λ), and blade pitch angles (θ). Using these nondimensional coefficients, the aerodynamic forces, thrust (F_a) and torque (T_a), can be calculated as:

$$F_a = \frac{1}{2} \cdot \rho_{air} \cdot A_R \cdot C_T(\lambda, \beta) \cdot v_{rel}^2 \quad [8]$$

$$T_a = \frac{1}{2} \cdot \rho_{air} \cdot A_R \cdot \frac{C_P(\lambda, \beta)}{\Omega} \cdot v_{rel}^3 \quad [9]$$

Where ρ_{air}, A_R, v_{rel} are the air density, rotor swept area and relative rotor windspeed, respectively. The relative rotor windspeed is calculated as the incoming windspeed (v_w) reduced by the hub motion velocity (v_{hub}):

$$v_{rel} = v_w - v_{hub} \quad [10]$$

4.2.3. Hydrodynamic model

As the presented model is intended for design optimization considering the wind turbine control optimization, it focuses on the wind turbine's operational range together with the sea conditions. The linear potential flow theory through a panel code software is applied in a previous computational step to solve the radiation-diffraction problem [35,36] for different floater model dimensions.

The hydrodynamic model for the reduced model in the tool is provided by the frequency-dependent added mass and radiation damping coefficients for various floater dimensions. Additionally, the hydrostatic restoring matrix, which incorporates contributions from the buoyancy centre (CB) and waterplane area, as well as the wave excitation force, is also obtained from the panel code solver for each of the floater designs in the same pre-process step.

The proposed tool's hydrodynamic module includes the calculation of the time-domain hydrodynamic radiation force, which accounts for the combined effect of added mass and radiation damping. This calculation incorporates the free surface memory effect by considering the convolution integral of the retardation function. This effect takes into account the delayed response of the water surface to the motion of the structure [31]. The validity of this approach, which is based on potential flow theory, was confirmed through validation studies conducted in Ref. [37]. The results obtained from these validation studies demonstrate the accuracy and reliability of the proposed approach in capturing the hydrodynamic behaviour of the system. The added mass and radiation damping time expressions are as follows:

$$\boldsymbol{A}_{\infty} = a(\omega) + \int_0^{\infty} B(\tau) \cdot \sin(\omega \tau) \mathrm{d}t \quad [11]$$

$$\boldsymbol{B}(\boldsymbol{\tau}) = \frac{2}{\pi} \cdot \int_0^{\infty} b(\omega) \cdot \cos(\omega \tau) \mathrm{d}\omega \quad [12]$$

$a(\omega)$ and $b(\omega)$ are the frequency dependant added mass and damping hydrodynamic coefficients. $B(\tau)$ is the retardation function calculated as a cosine transformation of the impulse response of the radiation function. With this added mass and radiation damping terms, the radiation force is calculated:

$$\boldsymbol{F}_{rad} = \boldsymbol{A}_{\infty} \cdot \ddot{\boldsymbol{q}} + \int_{-\infty}^{t} \boldsymbol{B}(\boldsymbol{t} - \boldsymbol{\tau}) \cdot \dot{\boldsymbol{q}}(\boldsymbol{\tau}) \mathrm{d}t \quad [13]$$

Similar to the hydrodynamic model in OpenFAST, the one implemented in the proposed tool offers the flexibility to incorporate linear stiffness matrices, linear damping matrices, and quadratic damping matrices. These matrices can be defined based on prototype tests or other experimental data [38].

The hydrodynamic module for the reduced nonlinear model in the proposed tool takes into account both first-order wave-excitation loads and second-order wave-excitation loads [31]. This is particularly important in FOWT systems, where significant slow-drift motions can occur impacting surge motion especially. The wave load can be calculated as the linear sum of first-order (F_{wave1}) and second-order loads (F_{wave2}):

$$\boldsymbol{F}_{exc} = \boldsymbol{F}_{wave1} + \boldsymbol{F}_{wave2} \quad [14]$$

The total first-order wave load can be decomposed into various wave-frequency load components, which are superimposed to represent the contributions of different wave frequencies:

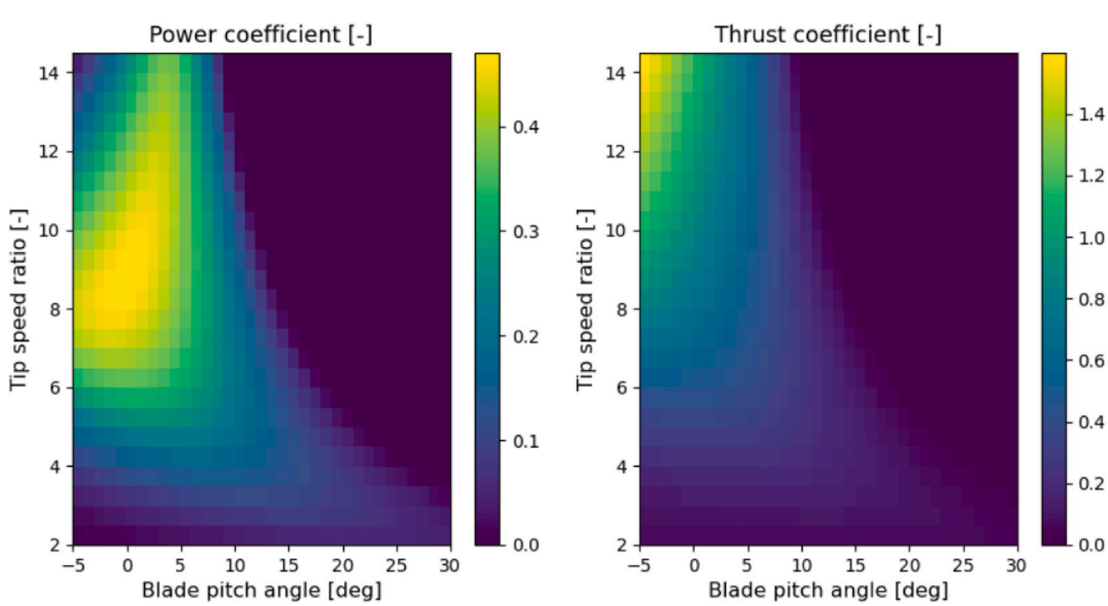

Fig. 4. Power and thrust coefficients.

$$\boldsymbol{F}_{\boldsymbol{wave1}} = \mathrm{Re}\left(\sum_{k=1}^{N} A_k \cdot \boldsymbol{X}(\boldsymbol{\omega}_k) \cdot e^{j\omega_k t}\right) \quad [15]$$

Where the complex incoming wave amplitude is represented by A_k. The normalised first-order wave-excitation force, $X(\omega_k)$ is related with the platform shape, wave frequency (ω_k) and wave direction. The $X_i(\omega_k)$ is obtained with the panel code software.

The second-order wave loads, like the first-order wave loads, are frequency dependent. These loads can be divided into sum- and difference-frequency incoming waves combinations. These pairs represent the combined effects of waves with different frequencies interacting with each other. The calculation of these second-order wave loads takes into account the nonlinear interactions between the waves, resulting in additional forces acting on the system.

The iteration leads to the generation of difference-frequency ($|\omega_k - \omega_l|$) and sum-frequency loads ($|\omega_k + \omega_l|$). The difference-frequency loads are particularly significant as they excite slow-drift motions in slack-moored structures and contribute to the induced wave mean-drift loads. These loads are especially relevant for platforms with soft mooring systems, such as catenary moorings, which typically have long natural periods. Fixed-bottom monopile or jacket foundations, as well as tension-leg floating platforms, are primarily affected by sum-frequency combinations due to the larger stiffness of the system [39].

The second-order excitation load comprises a non-zero mean component referred to as the mean-drift load. This mean-drift load is a result of the quadratic interactions in the first-order problem and thus, does not require solving the second-order potential problem. The mean drift excitation load can be mathematically represented by a quadratic transfer function (QTF) as follows:

$$\boldsymbol{F}_{\boldsymbol{drift}} = \mathrm{Re}\left(\sum_{k=1}^{N} A_k \cdot A_k \cdot \boldsymbol{X}^{\boldsymbol{drift}}(\omega_k) \cdot e^{j\omega_k t}\right) \quad [16]$$

In the implemented hydrodynamic model the Newman's approximation [40] is used to simplify the calculation of these forces. Newman's approximation method provides an estimation of the off-diagonal terms for the difference-frequency QTF based on the diagonal terms, see equation (15). By utilizing only, the mean-drift QTF derived from the first-order solution, it is possible to estimate the second-order difference-frequency behaviour. In other words, Newman's approximation allows to approximate the interaction between waves of different frequencies using the information obtained from the interaction with waves of a single frequency.

$$\begin{aligned}\boldsymbol{F}_{\boldsymbol{wave2}} = {} & \mathrm{Re}\left(\sum_{k=1}^{N} A_k \cdot \sqrt{2 \cdot X_i^-(\omega_k, \omega_k)} \cdot e^{j\omega_k t}\right)\Bigg|_{X_i^-(\omega_k,\omega_k)>0} \\ & - \mathrm{Re}\left(\sum_{k=1}^{N} A_k \cdot \sqrt{-2 \cdot X_i^-(\omega_k, \omega_k)} \cdot e^{j\omega_k t}\right)\Bigg|_{X_i^-(\omega_k,\omega_k)<0}\end{aligned} \quad [17]$$

4.2.4. Mooring system model

FOWT systems are anchored to the seabed by the mooring system. The system provides a restoring force based on the system position, see equation (18). To ensure computational efficiency within reasonable limits for optimization, certain assumptions are made. In this case, the forces arising from inertia, viscous drag, internal damping, bending, and torsion modes are disregarded. Instead, a quasi-static analysis approach is employed to determine the nonlinear catenary stiffness as a function of the platform movement. The validity of the proposed approach has been demonstrated in previous studies [41], confirming its effectiveness and reliability for floating substructures.

$$\boldsymbol{F}_{\boldsymbol{moor}} = \boldsymbol{F}_{\boldsymbol{moor}}(u) \quad [18]$$

In the proposed tool, the reduced nonlinear FOWT model utilises the same mooring system module as the complex model. However, a pre-processing step is conducted to define the different nonlinear catenary stiffness matrices. These matrices are then stored in a look-up table, which is used to efficiently compute the mooring forces in each simulation step. This approach allows for faster and more accurate calculations of the mooring system dynamics in the reduced model.

5. Tool validation: discussion of the reduced and complex models for FOWT coupled simulations

In this section, a comprehensive dynamic comparison between the two models, the reduced model, and OpenFAST, is presented. The comparison is conducted using an open access IEA15MW wind turbine [42] and VolturnUS-S platform [43] models. The table below, Table 1, summarises the key characteristics of the FOWT system.

Various case scenarios are considered to evaluate and analyse the performance of the models under different conditions from Ref. [44]. The comparison includes assessments of key parameters such as structural responses, and control performance. The evaluated cases, along with their descriptions, are summarised in the Table 2 below:

5.1. Natural frequencies and decay tests

To determine the natural frequencies of the FOWT system, the eigenvalue problem outlined in equation (17) must be solved. This problem involves finding the eigenvalues and corresponding eigenvectors that satisfy the system's equations of motion. By solving this problem, the natural frequencies of the FOWT system can be obtained.

$$\left(-\{\omega_n^2\}[M] + [K]\right)\{\widehat{x}(\omega)\} = \{0\} \quad [18]$$

The accurate calculation of these natural frequencies is crucial for designing and optimizing the FOWT system to ensure its stability and performance during operation.

To determine the natural frequencies in OpenFAST, a power spectral density (PSD) analysis is performed on the decay test data to extract the damped natural frequency of the system. This approach allows for an accurate estimation of the system's natural frequencies considering the damping effects. In Table 3, a comparison of the natural frequencies obtained from the analysis is presented, demonstrating a close agreement between the calculated natural frequencies and those identified through OpenFAST.

Exploring the system's response in the absence of external forces requires processing free-decay time domain simulations with both dynamic models. To ensure a fair comparison between the proposed model and OpenFAST, identical initial conditions are set as inputs for both simulations. Fig. 5 illustrates the time-domain outputs for each degree of freedom (DOF) obtained from the simulations. By examining these results, the agreement between the proposed model and OpenFAST can be assessed.

The proposed model and OpenFAST results exhibit good agreement for this evaluation case. However, slight differences can be observed. The variations in the observed periods in the results are a consequence of the diverse modelling approaches utilised to represent the structural

Table 1
FOWT system properties.

Parameter	Value	Units
Turbine rating	15	[MW]
Platform type	Semisubmersible	[–]
Freeboard	15	[m]
Draft	20	[m]
FOWT system total mass	20093	[ton]
Platform mass	17839	[ton]
Tower mass	1263	[ton]
RNA mass	950	[ton]
Water depth	200	[m]
Mooring system	Three-line chain catenary	[–]

Table 2
Tool dynamic evaluation cases.

Case	Description	Windspeed ($v\ \left[\frac{m}{s}\right]$)	Wave height ($H_s\ [m]$)	Wave period ($T_p\ [s]$)
1	Natural frequencies and decay tests	–	–	–
2	FOWT system response amplitude operators (RAOs)	–	–	–
3	Irregular waves no wind	–	0.3	3
4	Turbulent wind no waves	22.59	–	–
5	Irregular waves turbulent wind above rated	22.59	13.81	14.98

Table 3
FOWT system natural frequencies.

Degree of Freedom	Frequencies (Hz)		Periods (s)		Relative error [%]
	Reduced Model	OpenFAST	Reduced Model	OpenFAST	
Surge	0.0078	0.0074	127.76	134.47	4.99
Pitch	0.0359	0.0349	27.89	28.63	2.60
1st tower fore–aft mode	0.5243	0.5182	1.91	1.93	1.15

dynamics, with particular focus on the low number of DOFs considered in the reduced model. Furthermore, the differences in natural frequencies are primarily attributed to the mooring dynamics model used for the reduced model, which arises from employing a linear approximation of the mooring force based solely on the system's surge displacement while the complex model solves the catenary equation in each time step. Additionally, a higher damping value is evident for the fore-aft displacement in the reduced FOWT model due to disparities in the structural damping. This discrepancy arises from the constraint imposed by the modal shape function utilised to represent the tower's fore-aft flexible mode.

5.2. Response amplitude operators

To ensure an accurate representation of the system's response to wave forces, the system's RAOs are obtained in the absence of wind forces. The frequency domain equation of motion is derived from equation (6), as shown below:

$$\left(-\omega^2[M]+i\omega[C]+[K]\right)\{x(\omega)\}=\{F_w(\omega)\} \quad [19]$$

By solving this equation in frequency domain, the RAO of the FOWT system is obtained for the different floating DOFs. The RAO describes the structural response at a given frequency when subjected to a specific force, in this case waves. After solving this equation in frequency domain, simulations in time domain with regular waves of unit amplitude are carried out in OpenFAST to get the maximum value and compare it with the frequency solution as shown in Fig. 6.

5.3. Irregular waves no wind

A real sea state consists of non-uniform waves, and it is important to analyse the effects of such conditions on the FOWT system. To assess the system's response in a realistic environment, an irregular wave load case is introduced, excluding any wind load. This allows for a comprehensive evaluation of the hydrodynamic module of the tool.

In order to ensure consistent and comparable results, the same irregular wave elevation time series is used across the models. This allows for a direct comparison of the system's hydrodynamic loading conditions. The hydrodynamic loads generated in both models for these irregular wave conditions are depicted in Fig. 7.

The outcomes from cases 2 and 3 serve for validating and evaluating the hydrodynamics discrepancies. The frequency components of the responses exhibit a strong alignment between models. Similarly, the load generation shows a notable agreement during irregular wave conditions. However, minor discrepancies can be observed in the frequency response. At low wave frequency range the reduced model exhibits higher damping values, leading to the same conclusion depicted with the decay tests. Above a specific frequency value, each of the DOFs exhibits different frequency value, the responses of the complex model and reduced model curves differ one from the other due to the nonlinearities that OpenFAST accounts for that are not included in the reduced model.

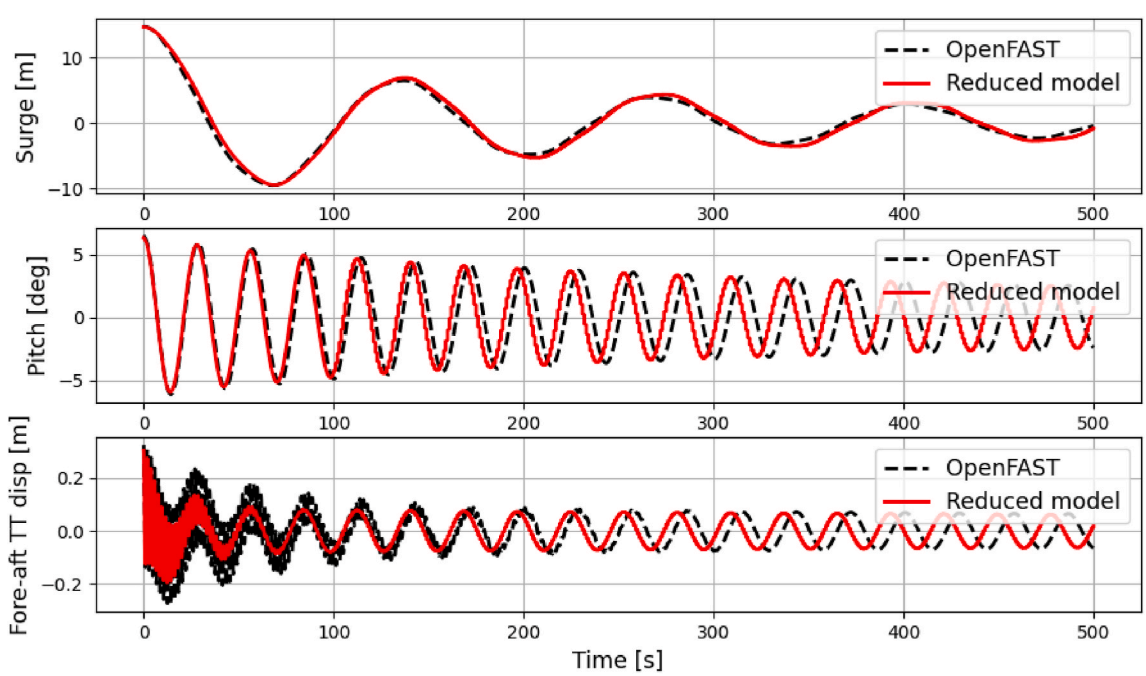

Fig. 5. Decay test comparison.

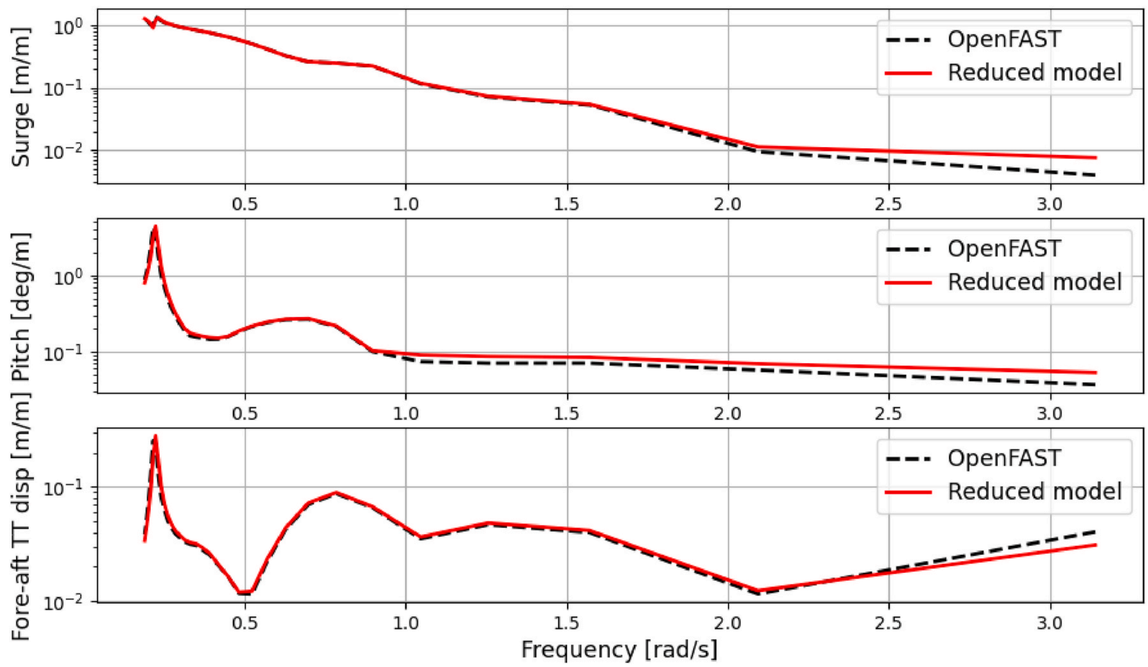

Fig. 6. System RAOs.

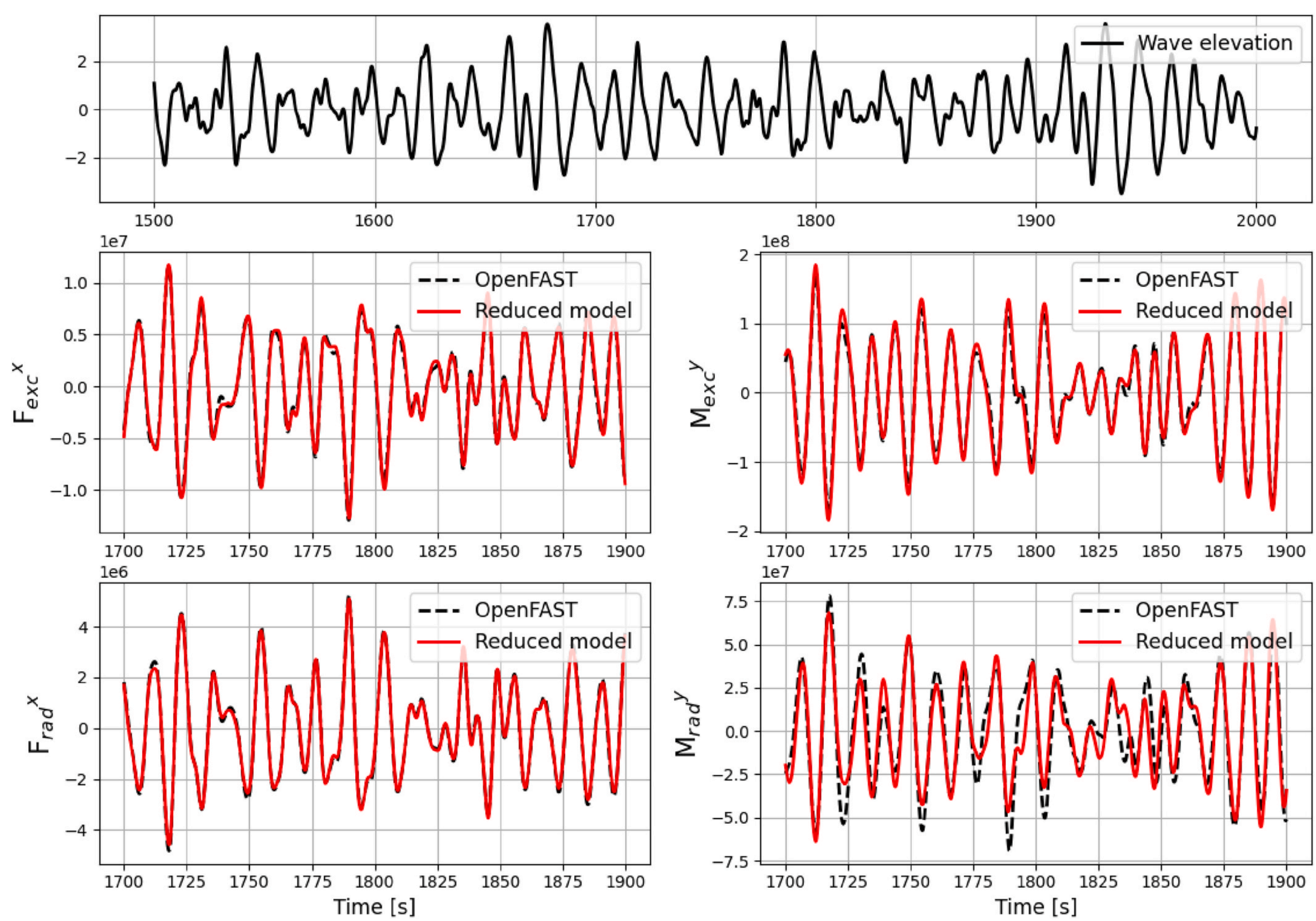

Fig. 7. Irregular wave load comparison.

The higher differences can be observed at high wave frequencies due to the limited DOFs included in the reduced model. When simulating the response in the time domain, the same conclusions can be obtained.

5.4. Turbulent wind still water

To assess the aerodynamic module's performance, a specific evaluation case is formulated, emphasizing the comparison of aerodynamic forces. The objective is to quantify the suitability of the integrated aerodynamic model within the tool. Both the aerodynamic thrust force and torque are calculated using both OpenFAST and the reduced model, ensuring they are subjected to the same conditions. Those loads are depicted in Fig. 8:

Case 4 serves as a validation test for the aerodynamic model utilised in the proposed model. The aerodynamic forces obtained from both the proposed model and OpenFAST exhibit good agreement for the turbulent wind conditions in the absence of waves. However, there are slight discrepancies that can be observed. These variations are likely the result of the simplifications applied to the aerodynamic loading representation within the reduced model. However, it's important to note that despite these slight differences, the validation results affirm the competence of the aerodynamic model utilised in the proposed framework.

5.5. Irregular waves turbulent wind

The last load case intends to showcase all the functionalities offered by the proposed tool once the validation of the reduced FOWT system model is accomplished. Fig. 9 illustrates the profile of turbulent wind speed and wave elevation utilised for this demonstration. These profiles are crucial for precisely capturing the wind turbine's dynamic behaviour under real-world operational conditions and serve as an exemplification of the capabilities of the proposed tool.

In this load case, some of the implemented controllers are tested within the tool environment. By activating the controller, the wind turbine system can respond dynamically to the turbulent wind speed and wave elevation, simulating its behaviour in an actual operational scenario. This load case provides valuable insights into the proposed tool performance under realistic operating conditions, Fig. 10.

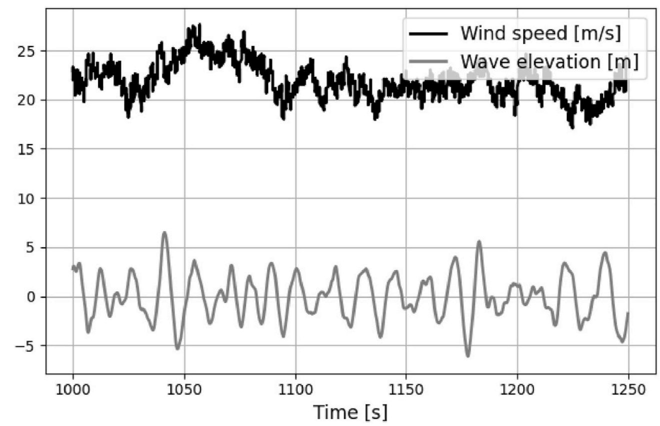

Fig. 9. Turbulent wind and irregular wave time series.

This final validation test aims to present the capacities of the developed tool to simulate the FOWT system under conditions that closely resemble real operation. Irregular waves and turbulent wind are applied to assess the system's response while operating the wind turbine with different controllers. In this particular scenario, both dynamic models have been employed in isolation to effectively showcase the comprehensive functionalities and the inherent modularity of the tool. The simulations utilizing the reduced order model encompass the implementation of a NMPC strategy. In contrast, with OpenFAST, a feedback control loop encompassing two distinct loops is activated, comprising the baseline detuned control loop along with a damper loop.

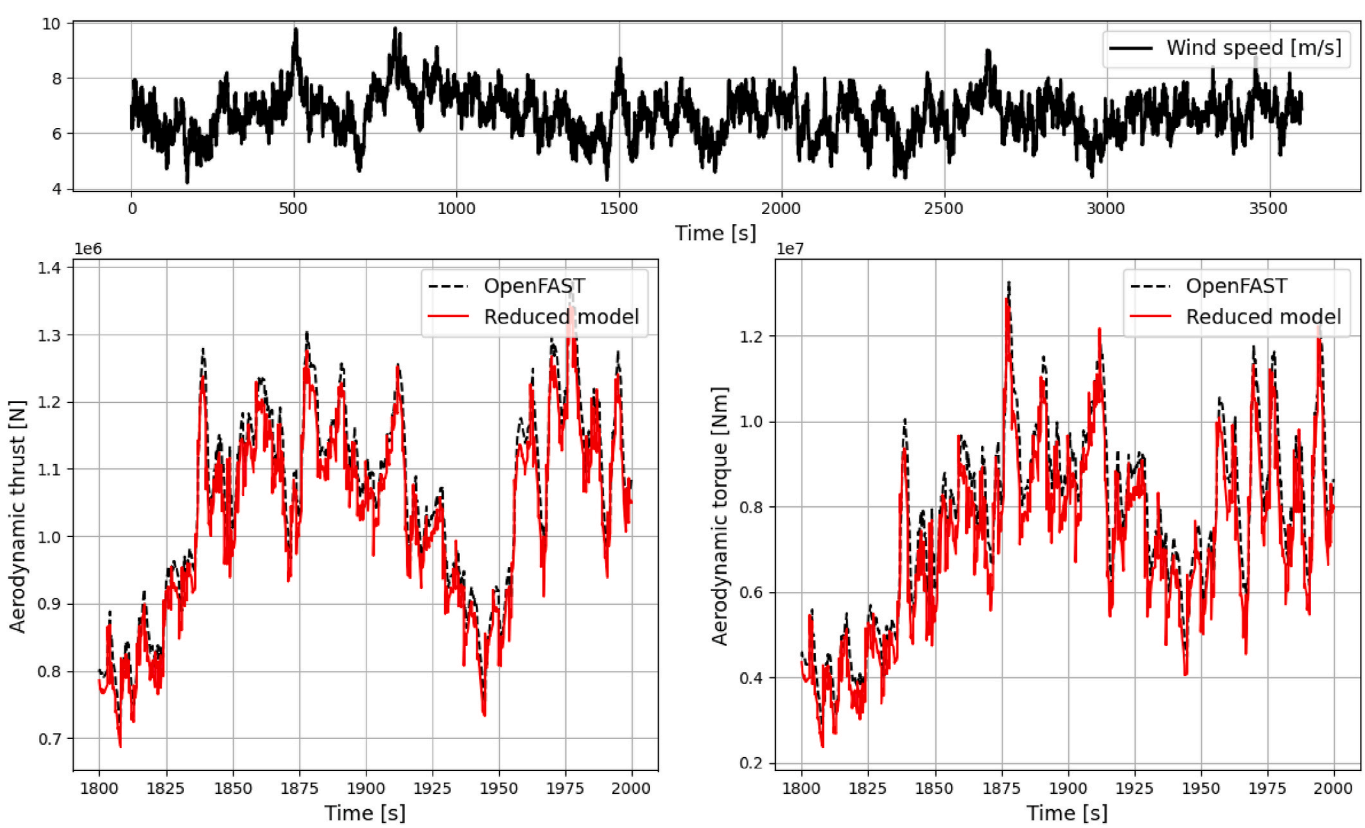

Fig. 8. Aerodynamic loads comparison.

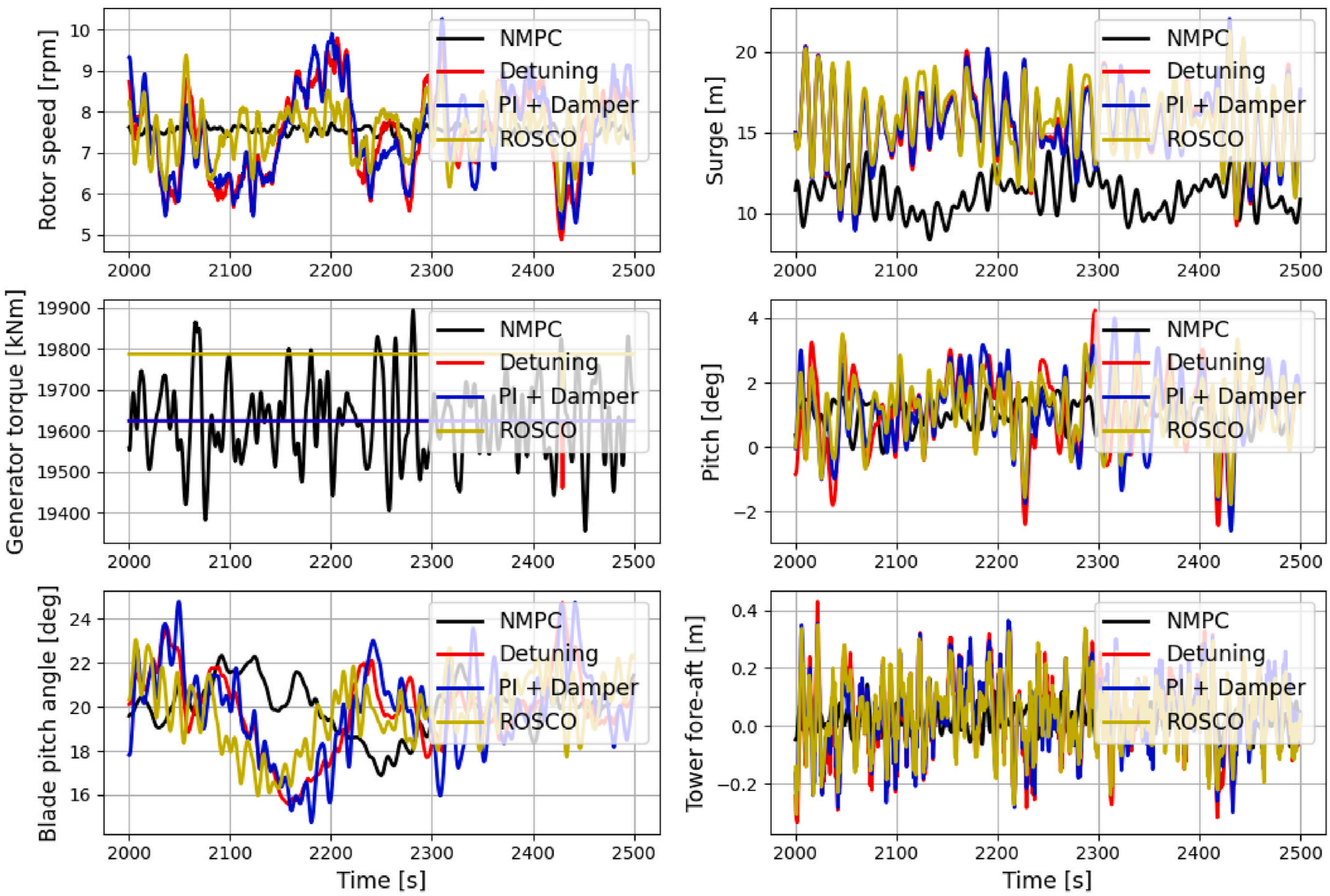

Fig. 10. System and controller response.

Additionally, a final simulation is conducted employing OpenFAST and ROSCO, effectively demonstrating that not only the developed controllers can be seamlessly integrated within the tool but also well-established state-of-the-art tools.

Upon careful examination, it becomes evident that all the responses are consistently aligned within the same order of magnitude, thereby affirming the proposed tool's capability to adequately respond to realistic environmental conditions. However, noteworthy discrepancies emerge when comparing the responses generated by the NMPC controller with those produced by other controllers, particularly in the utilization of generator torque. This discrepancy arises due to the nuanced control strategies implemented in each of the controllers.

The results garnered from this comprehensive evaluation serve to stimulate further development of the tool. The identified variations, particularly in the context of controller behaviours, underscore the need to explore the incorporation of optimization procedures for both the controller and the FOWT system itself. These results provide a compelling impetus for enhancing the tool's versatility and effectiveness, enabling more refined and optimised wind turbine system designs in the future.

6. Conclusions

The paper introduces a novel Python-based tool for simulating FOWT systems. This tool provides users with the flexibility to select from a range of controllers and complexity models, offering various options for system analysis and evaluation. The reduced model's rapid analysis time accelerates the early design stage compared to using a more complex simulation time domain model such as OpenFAST, enabling swift implementation of necessary modifications to the model, the controller, or both. Incorporating a higher complexity model enables the evaluation, validation, and verification of changes within a more sophisticated simulation environment. Continuing in this vein, the tool also provides a straightforward means to incorporate optimization routines for the model, the controller, or both, making it suitable as a framework for developing CCD methodologies. This has been addressed by assuming a complete FOWT system optimised design and evaluating the response of the system in each of the available models. In upcoming tool versions, the authors intend to integrate optimization capabilities into the tool for platform, moorings, and tower designs. Additionally, autotuning procedures for the controllers will be introduced, granting users the ability to define the cost function for the optimization process.

Financial disclosure

The work was funded by the Basque Government through the BIKAINTEK PhD support program (grant no. 48-AF-W2-2019-00010), and through the Elkartek program (grant no. KK-2022/00090, KONFLOT project). The authors acknowledge NAUTILUS Floating Solutions for their support to the PhD thesis of Javier Lopez-Queija. The research has been carried out within the framework of the Joint Research Laboratory on Offshore Renewable Energy (JRL-ORE). The authors also acknowledge EUSKAMPUS FUNDAZIOA for their support through the Misiones 1.0 program.

CRediT authorship contribution statement

Javier López-Queija: Conceptualization, Formal analysis, Investigation, Methodology, Software, Supervision, Validation, Writing – original draft, Writing – review & editing. **Eneko Sotomayor:**

Conceptualization, Software. **Josu Jugo:** Conceptualization, Methodology, Software, Supervision. **Ander Aristondo:** Software. **Eider Robles:** Project administration, Resources, Supervision.

Declaration of competing interest

The authors declare that they have no known competing financial interests or personal relationships that could have appeared to influence the work reported in this paper.

Acknowledgments

The work was funded by the Basque Government through the BIKAINTEK PhD support program (grant no. 48-AF-W2-2019-00010), and through the Elkartek program (grant no. KK-2022/00090, KONFLOT project). The authors acknowledge NAUTILUS Floating Solutions for their support to the PhD thesis of Javier Lopez-Queija. The research has been carried out within the framework of the Joint Research Laboratory on Offshore Renewable Energy (JRL-ORE). The authors also acknowledge EUSKAMPUS FUNDAZIOA for their support through the Misiones 1.0 program.

References

[1] Center for Sustainable Systems, University of Michigan, Wind Energy Factsheet, Pub. No. CSS07-09, 2021.
[2] Global Wind Energy Council (GWEC), Global Wind Report, 2023.
[3] A. Martinez, G. Iglesias, Mapping of the levelised cost of energy for floating offshore wind in the European Atlantic, Renew. Sustain. Energy Rev. 154 (2022) 111889, https://doi.org/10.1016/j.rser.2021.111889.
[4] A.P. Deshmukh, J.T. Allison, Multidisciplinary dynamic optimization of horizontal axis wind turbine design, Struct. Multidiscip. Optim. 53 (2016) 15–27, https://doi.org/10.1007/s00158-015-1308-y.
[5] M. Garcia-Sanz, Control Co-Design: an engineering game changer, Adv Control Appl 1 (2019) e18, https://doi.org/10.1002/adc2.18.
[6] P. Bortolotti, C. Bay, G. Barter, E. Gaertner, K. Dykes, M. McWilliam, M. Friis-Moller, M. Molgaard Pedersen, F. Zahle, System Modeling Frameworks for Wind Turbines and Plants: Review and Requirements Specifications, 2022, https://doi.org/10.2172/1868328.
[7] J. Jonkman, A. Wright, G. Barter, M. Hall, J. Allison, D.R. Herber, Functional requirements for the WEIS toolset to enable controls Co-design of floating offshore wind turbines, in: ASME 2021 3rd International Offshore Wind Technical Conference, American Society of Mechanical Engineers, Virtual, Online, 2021 V001T01A007, https://doi.org/10.1115/IOWTC2021-3533.
[8] WISDEM ® Documentation — WISDEM 2.0 documentation, (n.d.). https://wisdem.readthedocs.io/en/master/(accessed July 11, 2023).
[9] NREL: WISDEM, (n.d.). https://github.com/WISDEM (accessed July 11, 2023)..
[10] OpenFAST Documentation — OpenFAST v3.5.0 documentation, (n.d.). https://openfast.readthedocs.io/en/main/index.html (accessed July 11, 2023) .
[11] NREL: OpenFAST, GitHub. (n.d.). https://github.com/OpenFAST (accessed July 11, 2023)..
[12] A.K. Sundarrajan, Y.H. Lee, J.T. Allison, D.R. Herber, Open-loop control Co-design of floating offshore wind turbines using linear parameter-varying models, in: Volume 3A: 47th Design Automation Conference (DAC), American Society of Mechanical Engineers, Virtual, Online, 2021 V03AT03A010, https://doi.org/10.1115/DETC2021-67573.
[13] J.M. Hegseth, E.E. Bachynski, J.R.R.A. Martins, Integrated design optimization of spar floating wind turbines, Mar. Struct. 72 (2020) 102771, https://doi.org/10.1016/j.marstruc.2020.102771.
[14] N. Abbas, D. Zalkind, L. Pao, A. Wright, A Reference Open-Source Controller for Fixed and Floating Offshore Wind Turbines, Control and System Identification, 2021, https://doi.org/10.5194/wes-2021-19.
[15] NREL: Reference OpenSource Controller (ROSCO) toolbox for wind turbine applications, (2023). https://github.com/NREL/ROSCO (accessed July 11, 2023)..
[16] J. Jonkman, Influence of control on the pitch damping of a floating wind turbine, in: 46th AIAA Aerospace Sciences Meeting and Exhibit, American Institute of Aeronautics and Astronautics, Reno, Nevada, 2008, https://doi.org/10.2514/6.2008-1306.
[17] G.J. van der Veen, I.J. Couchman, R.O. Bowyer, Control of floating wind turbines, in: ACC, Montreal, Canada, 2012, pp. 3148–3153.
[18] J. López-Queija, E. Robles, J. Jugo, S. Alonso-Quesada, Review of control technologies for floating offshore wind turbines, Renew. Sustain. Energy Rev. 167 (2022) 112787, https://doi.org/10.1016/j.rser.2022.112787.
[19] F.D. Bianchi, H. De Battista, R.J. Mantz, Wind Turbine Control Systems: Principles, Modelling and Gain Scheduling Design, Springer, London, 2007.
[20] W. Yu, F. Lemmer, D. Schlipf, P.W. Cheng, B. Visser, H. Links, N. Gupta, S. Dankemann, B. Counago, J. Serna, Evaluation of control methods for floating offshore wind turbines, J. Phys.: Conf. Ser. 1104 (2018) 012033, https://doi.org/10.1088/1742-6596/1104/1/012033.
[21] F. Lemmer, né Sandner, W. Yu, D. Schlipf, P.W. Cheng, Robust gain scheduling baseline controller for floating offshore wind turbines, Wind Energy 23 (2020) 17–30, https://doi.org/10.1002/we.2408.
[22] T.J. Larsen, T.D. Hanson, A method to avoid negative damped low frequent tower vibrations for a floating, pitch controlled wind turbine, J. Phys.: Conf. Ser. 75 (2007) 012073, https://doi.org/10.1088/1742-6596/75/1/012073.
[23] D. Schlipf, E. Simley, F. Lemmer, L. Pao, P.W. Cheng, Collective pitch feedforward control of floating wind turbines using lidar, Journal of Ocean and Wind Energy 2 (2015), https://doi.org/10.17736/jowe.2015.arr04.
[24] H.G. Bock, K.J. Plitt, A multiple shooting algorithm for direct solution of optimal control problems, IFAC Proc. Vol. 17 (1984) 1603–1608, https://doi.org/10.1016/S1474-6670(17)61205-9.
[25] G. Frison, M. Diehl, HPIPM: a high-performance quadratic programming framework for model predictive control, IFAC-PapersOnLine 53 (2020) 6563–6569, https://doi.org/10.1016/j.ifacol.2020.12.073.
[26] R. Verschueren, G. Frison, D. Kouzoupis, J. Frey, N. van Duijkeren, A. Zanelli, B. Novoselnik, T. Albin, R. Quirynen, M. Diehl, acados—a modular open-source framework for fast embedded optimal control, Mathematical Programming Computation 14 (2022) 147–183, https://doi.org/10.1007/s12532-021-00208-8.
[27] acados — acados documentation, (n.d.). https://docs.acados.org/index.html (accessed July 11, 2023).
[28] J. López-Queija, E. Robles, J.I. Llorente, I. Touzon, J. López-Mendia, A simplified modeling approach of floating offshore wind turbines for dynamic simulations, Energies 15 (2022) 2228, https://doi.org/10.3390/en15062228.
[29] T. Burton (Ed.), Wind Energy: Handbook, J. Wiley, Chichester ; New York, 2001.
[30] M. Paz, Y.H. Kim, Structural Dynamics: Theory and Computation, Springer International Publishing, Cham, 2019, https://doi.org/10.1007/978-3-319-94743-3.
[31] J.M.J. Journeé, W.W. Massie, Offshore Hydromechanics, 2001. Delft.
[32] M. Karimirad, Offshore Energy Structures: for Wind Power, Wave Energy and Hybrid Marine Platforms, Springer International Publishing, Cham, 2014, https://doi.org/10.1007/978-3-319-12175-8.
[33] M. Masciola, J. Jonkman, A. Robertson, Implementation of a Multisegmented, Quasi-Static Cable Model, (n.d.)..
[34] F. Lemmer, D. Schlipf, P.W. Cheng, Control design methods for floating wind turbines for optimal disturbance rejection, J. Phys.: Conf. Ser. 753 (2016) 092006, https://doi.org/10.1088/1742-6596/753/9/092006.
[35] Det Norske Veritas, DNV-OS-J101: Design of Offshore Wind Structures, Det Norske Veritas, Havik, Norway, 2014. http://www.ffbww.com/pdf/32.pdf. (Accessed 29 January 2015).
[36] T.I. Fossen, Handbook of Marine Craft Hydrodynamics and Motion Control, John Wiley & Sons, Hoboken, USA, 2011.
[37] I. Touzon, V. Nava, Z. Gao, I. Mendikoa, V. Petuya, Small scale experimental validation of a numerical model of the HarshLab2.0 floating platform coupled with a non-linear lumped mass catenary mooring system, Ocean Eng. 200 (2020) 107036, https://doi.org/10.1016/j.oceaneng.2020.107036.
[38] A. Otter, J. Murphy, V. Pakrashi, A. Robertson, C. Desmond, A review of modelling techniques for floating offshore wind turbines, Wind Energy 25 (2022) 831–857, https://doi.org/10.1002/we.2701.
[39] T.M. Duarte, A.J. Sarmento, J.M. Jonkman, Effects of second-order hydrodynamic forces on floating offshore wind turbines, in: 32nd ASME Wind Energy Symposium, American Institute of Aeronautics and Astronautics, National Harbor, Maryland, 2014, https://doi.org/10.2514/6.2014-0361.
[40] J.N. Newman, Second-order, Slowly-Varying Forces on Vessels in Irregular Waves, 1974. London, UK.
[41] I. Touzon, V. Nava, B. de Miguel, V. Petuya, A comparison of numerical approaches for the design of mooring systems for wave energy converters, J. Mar. Sci. Eng. 8 (2020) 523, https://doi.org/10.3390/jmse8070523.
[42] E. Gaertner, J. Rinker, L. Sethuraman, F. Zahle, B. Anderson, G. Barter, N. Abbas, F. Meng, P. Bortolotti, W. Skrzypinski, G. Scott, R. Feil, H. Bredmose, K. Dykes, M. Shields, C. Allen, A. Viselli, Definition of the IEA 15-Megawatt Offshore Reference Wind, National Renewable Energy Laboratory, Golden, CO, 2020. https://www.nrel.gov/docs/fy20osti/75698.pdf.
[43] C. Allen, A. Viscelli, H. Dagher, A. Goupee, E. Gaertner, N. Abbas, M. Hall, G. Barter, Definition of the UMaine VolturnUS-S Reference Platform Developed for the IEA Wind 15-Megawatt Offshore Reference Wind Turbine, 2020, https://doi.org/10.2172/1660012.
[44] J. Berque, LIFE50+: Qualification of innovative floating substructures for 10MW wind turbines and water depths greater than 50m: Oceanographic and meteorological conditions for the design, n.d. https://lifes50plus.eu/wp-content/uploads/2015/12/GA_640741_LIFES50-_D1.1.pdf..